NASA TECHNICAL MEMORANDUM

NASA TM X-52416

NASA TM X-52416

EXPERIMENTAL STABILITY STUDIES OF THE HERRINGBONE-GROOVED GAS LUBRICATED JOURNAL BEARING

by Robert E. Cunningham, David P. Fleming, and William J. Anderson
Lewis Research Center
Cleveland, Ohio

TECHNICAL PAPER proposed for presentation at Second International Symposium on Gas Lubrication, Design, and Application and Exhibit sponsored by the American Society of Mechanical Engineers and the Office of Naval Research
Las Vegas, Nevada, June 17-20, 1968

NATIONAL AERONAUTICS AND SPACE ADMINISTRATION · WASHINGTON, D.C. · 1968

EXPERIMENTAL STABILITY STUDIES OF THE HERRINGBONE-GROOVED GAS LUBRICATED JOURNAL BEARING

by Robert E. Cunningham, David P. Fleming,
and William J. Anderson

Lewis Research Center
Cleveland, Ohio

TECHNICAL PAPER proposed for presentation at

Second International Symposium on Gas Lubrication,
Design, and Application and Exhibit
sponsored by the American Society of Mechanical Engineers
and the Office of Naval Research
Las Vegas, Nevada, June 17-20, 1968

NATIONAL AERONAUTICS AND SPACE ADMINISTRATION

EXPERIMENTAL STABILITY STUDIES OF THE HERRINGBONE-GROOVED GAS LUBRICATED JOURNAL BEARING

by Robert E. Cunningham, David P. Fleming, and William J. Anderson

Lewis Research Center
National Aeronautics and Space Administration
Cleveland, Ohio

E-3992

ABSTRACT

Experimental studies were conducted on six rotors, $1\frac{1}{2}$-inches diameter by $12\frac{1}{4}$-inches long operating in ambient air to high compressibility numbers. Herringbone-groove geometries and clearances were varied to determine their effect on half frequency whirl (HFW). All rotors were operated vertically and without any applied radial load. Results show that half frequency whirl onset is very sensitive to radial clearance. Limited test results indicate that a fully grooved bearing is more stable than a partially grooved one, other parameters being equal. Generally fair agreement between theory and experiment was achieved for predicting HFW onset speeds.

SYMBOLS

a_g	width of helical groove, in.
a_r	width of helical land, in.
C	bearing radial clearance, in.
D	rotor diameter, in.
F_r	radial bearing force, lb
F_t	tangential force, lb

TM X-52416

e	rotor eccentricity, in.
h_g	groove clearance, in.
h_r	ridge clearance, in.
H	ratio groove clearance to ridge clearance, h_g/h_r
L	bearing length, in.
L_1	length of grooved portion of bearing, in.
M	mass of rotor per bearing, (lb)(sec^2)/in.
$\overline{M}$	dimensionless mass parameter, $MP_aR/\mu^2LD[(C/R)^5]$
N	shaft speed, rpm
N_s	half frequency whirl onset speed, rpm
n	number of grooves
P_a	atmosphere pressure, lb/in.^{2} absolute
R	rotor radius, in.
W	total weight of rotor, lb
Y	ratio of grooved portion of bearing length, L_1/L
α	ratio of groove width ot total width, groove plus land, $a_g(a_g + a_r)$
β	helix angle, deg
ϵ	journal eccentricity ratio, e/C
ω	angular rotor speed, rad/sec
δ	groove depth, in.
Λ	compressibility number, $(6\mu\omega/P_a)(R/C)^2$
μ	absolute viscosity, (lb)(sec)/in.^{2}

INTRODUCTION

Space turbomachinery of the type used in a closed loop, Brayton Gas Cycle must be compact and lightweight. If the cycle gas is used as a lubricant these machines are more compact and lighter than machines using oils as lubricants. Components like oil pumps, contact seals, oil scavenging and separating systems normally required with conventionally lubricated bearings, are elimenated (ref. 1). A reduction in parasitic losses is an additional advantage gained by eliminating these auxiliary components.

A closed loop cycle is one in which an inert gas is continuously recirculated. If the system is to operate reliably for many thousands of hours, this cycle gas must remain clean. Gas bearings are well suited to this application. Their use precludes the possibility of working fluid contamination since there is no direct contact of shaft and bearing during normal operation (ref. 2).

The shafts of any turbomachine running in fluid film bearings generally experience two types of instability. The first is a synchronous vibration due to unbalance of the rotating masses. The second, and much more serious, is a self excited nonsynchronous vibration. Lightly loaded rotors operate with high attitude angles and small eccentricity ratios. Under these conditions the tangential component of the pressure force is quite large. The resulting moment drives the rotor in an orbital path about the bearing center and in the direction of rotation. The frequency of this orbital motion is approximately one-half

that of the rotor speed and hence has been given the name Half-Frequency Whirl (HFW) (ref. 3).

Attempts to theoretically predict the onset of HFW have been the subject of many papers, three of which are referenced (refs. 4, 5, and 6). A difficult problem arises, however, in attempting to solve the time dependent Reynolds equation for compressible flow. The assumptions, necessary in even the most complex of mathematical models, limit the accuracy of resulst. It is necessary, therefore, to supplement the theoretical analysis with experimentation.

A numberof self-acting bearing designs have evolved that have somewhat stable operating characteristics. These designs shape the bearing surface to create artificial fluid film wedges in the absence of any applied radial load. Radial restoring forces are generated which tend to keep the journal from whirling. Listed in the order of least to most stable operation are: (1) Elliptical Bearing, (2) Three and Four Lobe Bearing, (3) Three and Four Sector Tilting Pad Bearing. References 7 and 8 give a more detailed analysis of their operating characteristics. All of these designs achieve a certain degree of stability, but at the expense of load capacity. An additional disadvantage of the tilting pad bearing is its complexity. Each shoe is independently mounted on a pivot. This allows each shoe to pivot and thus conform to the rotor attitude. In addition, some method of adjustment is usually required on at least one of the shoe to obtain alinement at assembly.

The helical grooved, or the herringbone-grooved bearing, shows the most promise of stable operation with no sacrifice in load capacity, (refs. 9 and 10). Shallow grooves formed in a herringbone pattern act like a viscous pump when the shaft turns (see figs. 1(a) and (b)). Air is pumped from the bearing ends toward the middle. The pressure distribution that results is similar to that obtained in a hydrostatic bearing. Herringbone-grooved bearings operating at large compressibility numbers have small attitude angles much like those of a hydrostatic gas bearing. The small attitude angles tend to produce large radial restoring forces in both types of bearings. The difference, however, it that these restoring forces increase significantly with speed in the herringbone-grooved bearing.

The objectives of this study were to investigate experimentally (1) the stability characteristics of the herringbone-grooved gas-journal bearing to high compressibility numbers and (2) to compare the test results with existing stability theory (ref. 11). The following parameters and their effects on threshold of HFW were examined: (1) Helix angle (2) No. of grooves (3) partial and full grooving and (4) clearance.

Six rotors, $1\frac{1}{2}$ inches in diameter by $12\frac{1}{4}$ inches long equipped with two herringbone-grooved journals having varying geometries were tested to speeds of 60,830 RPM. The rotors were mounted in two cylindrical bronze sleeves and operated in a vertical position to negate gravity forces. The dynamic attitude of the rotors in the bearings was continuously monitored and whirl onset speeds recorded. Different

sets of bronze sleeves were used to determine the effects of clearance on whirl onset speeds.

APPARATUS

The apparatus used in conducting these tests is shown schematically in figure 2. A steel rotor $1\frac{1}{2}$ inches in diameter and $12\frac{1}{4}$ inches long is mounted vertically in two smooth cylindrical bronze sleeves. Two herringbone-grooved patterns in the rotor surface and centered in the bronze sleeves comprise the bearing assembly. Groove patterns extend beyond the end of the sleeves to insure a supply of ambient air. The sleeves are $1\frac{1}{2}$ inches long and the axial centerline distance between the two sleeves is $6\frac{5}{8}$ inches. An externally pressurized pocket thrust bearing supports the rotor at its lower end.

The rotors are driven by an impulse turbine assembly. It consists of ten 1/8 inch diameter nozzles and six equally speced turbine buckets machined into the rotor at its upper end. A solid state electronic controller was used to regulate the turbine air supply and thes accurately maintain a preset rotor speed.

Instrumentation

Two orthogonally oriented capacitance, distance probes were located in the same radial plane and outboard of each bearing. These probes provided a noncontacting method of detecting radial displacement of the rotor. A fifth capacitance probe mounted flush with the thrust bearing surface was used to monitor thrust bearing clearance.

An X-Y curve tracing Cathode Ray Oscilloscope (CRO) was used to display the signals generated by the probes of both upper and lower bearings. Either an orbital motion trace or a displacement-versus-time trace could be displayed.

TEST ROTORS

A total of six rotors having different groove geometries were evaluated and are listed in table I. Two of the six rotors tested, a partial and fully-grooved type are shown in the photographs and schematic drawings of figures 1(a) and (b), respectively.

Concentricity and roundness measurements were made by both the vendor and inspection personnel at NASA-Lewis. Although these measurements were made on two different types of geometry gages, agreement was considered good. Inspection of the charts made on each rotor showed roundness and concentricity averaged 20 microinches TIR. Diametral taper over the grooved portion of each rotor averaged 30 microinches, the maximum being 70 microinches. Diameters of rotors at midspan were larger than at the ends indicating a slight "barrel" shape to the rotors. These variations, however, were within print tolerances.

The aluminum bronze sleeves into which the herringbone-grooved rotors were assembled were in-line bored and lapped. The inside diameters were measured at several places along the sleeve using an air gage with accuracy of 10 microinches. Roundness, concentricity and taper of sleeves were as good or better than those of the rotors.

A typical surface profile trace made on two of the subsurface Herringbone-grooves is shown in figure 3. The average depths of grooves for each rotor are listed in table I.

PROCEDURE

Prior to assembly, the surface of each rotor was thoroughly cleansed with alcohol. After assembly of the rotor, clearances in two orthogonal planes, for both upper and lower bearings were measured using the calibrated capacitance probes and a digital voltmeter read-out. This was also done after each test. These clearances compared closely with previously measured bearing bore and rotor diameter measurements.

Each rotor was accelerated to speed and its synchronous whirl orbit noted. If the amplitude of unbalance was too large for any given rotor, this rotor was then balanced. This was done with the aid of a reference marker (flat spot on rotor directly under each capacitance probe). This reference marker occurs on the CRO amplitude-time trace once per revolution. The plane of maximum rotor excursion relative to the reference marker is easily determined.

After balancing, each rotor was then accelerated to speed and the threshold of HFW noted if and when it occurred. If HFW occurred, the speed was slowly increased beyond the threshold speed. The test was stopped if the whirl amplitude grew rapidly. If the amplitude remained small the speed was increased to the limiting speed of the air turbine drive.

RESULTS AND DISCUSSION

Experimental results obtained on six rotors with different groove geometries are shown in table I and in figures 4 through 8. The rotors were operated in air at standard conditions and up to a maximum bearing compressibility number of 45.

The decided influence of radial clearance on stability is readily apparent when comparing results of table I. For a radial clearance range of 550 to 710 microinches all five partially grooved rotors exhibited half frequency whirl (HFW). Whirl onset speed was the lowest for rotor A-5 which had the largest clearance of 710 microinches. The highest (HFW) threshold speed occurred with rotor A-1 at the smallest assembled radial clearance of 550 microinches. When the same five rotors were operated at clearances ranging from 370 to 500 microinches (table I) none of the rotors whirled up to a maximum speed of 59,000 rpm.. Helix angles and number of grooves were varied. Groove to land width ratio and groove length to overall length ratio were held constant for rotors A-1 through A-5. Rotor diameter, length, weight and bearing span were also held constant.

Figures 4(a) through (c) are pictures of the amplitude time trace of rotor A-1 running in the high clearance sleeves. HFW threshold speed was 27,900 rpm. At 30,000 rpm, the amplitude was 275 microinches. At 35,000 rpm the amplitude had increased to 413 microinches. A further increase in speed showed no additional growth of the whirl orbit. At a speed of 48,000 rpm, the shaft motion

became synchronous, having an amplitude of approximately 75 microinches. This low amplitude synchronous whirl was observed up to the maximum speed of 56,500 rpm, which was the upper limiting speed imposed by the air turbine drive.

Theory predicts that a fully grooved herringbone bearing of the type shown in the photograph figure 1(b) should be more stable than the partially grooved bearing of figure 1(a). To verify this, a fully grooved rotor designated B-1 was made which was to be identical to A-1 except for length of grooves. The vendor, however, experienced difficulty in fabricating the groove pattern in B-1; consequently, the grooves are considerably shallower than in A-1 (330 vs 580 microinches). In addition, B-1 was slightly larger in diameter, resulting in a clearance of 530 microinches for B-1, compared to 550 microinches for A-1. The slightly smaller clearance would marginally increase stability; however, theory predicts that the shallow grooves on B-1 should make that rotor considerably less stable than an equivalent rotor with the groove depth of A-1. Despite this, rotor B-1 was run to a speed of 60,830 rpm without any HFW being observed. It is concluded, therefore, that in addition to clearance, the length of grooves is an important factor in the stability of a bearing. Due to widely varying groove depths between upper and lower bearings on rotor B-1 attempt was made to compare the experimental data with a theoretical stability plot.

Figures 5 through 8 show a comparison of the experimental results with the theoretical. Shown in these stability plots is rotor mass parameter (dimensionless) versus compressibility number (also dimensionless). These curves are based on the work described in reference 11 and also briefly outlined in the Appendix of this report.

Neither of the two experimental curves of figure 5 intersect the theoretical HFW region. Rotor A-1 at a zero speed clearance of 550 microinches did, however operate in the HFW region. The HFW threshold speed observed was 27,900 rpm, corresponding to a compressibility number of 6.4. Return to stable operation occurred at a speed of 48,000 rpm, corresponding to a compressibility number of approximately 13. The lower experimental curve for rotor A-1 at a zero speed clearance of 370 inches falls far below the lowest portion of the HFW zone. The downward slope of the experimental curves is due to a decreasing clearance caused by centrifugal growth of the rotor. The amount of growth due to centrifugal effects was calculated.

Agreement between theory and experiment is generally fair as shown by test results in the composite plot of figure 6 for rotors A-1 through A-5 at high clearance values. Data is included in figure 6 for four rotors run in a third set of bronze sleeves having clearances larger than those listed in table I. As would be expected, the HFW occurred at relatively low speeds under these conditions. Based on these test results the actual zone of unstable operation is somewhat

smaller than that predicted by the theory. It should be pointed out, however, that some heating of the rotor and housing parts was observed during the test runs. Dimensional changes of the bronze sleeves and rotor could have resulted in larger clearances than were measured at the start of the tests. This would tend to raise the data points and result in better agreement. However, measurements made at the end of a test did now show any definite pattern of clearance change.

Entry into the theoretical HFW region at high dimensionless mass numbers, $\overline{M}$ not only occurs at a low threshold speed but in addition, produces a large amplitude whirl motion. This is shown by experimental results obtained for rotor A-2 and A-3 (fig. 7) and A-4 and A-5 (fig. 8) at high clearances. It was not possible to increase the speed much beyond the HFW threshold because of the rapid growth in the whirl orbit for small increases in speed. This was not the case with rotor A-1 (fig. 5) in the high clearance sleeves. Here it was possible to pass completely through the HFW region without experiencing an excessive whirl amplitude because of lower values of $\overline{M}$.

SUMMARY OF RESULTS

The results listed below were obtained with six $1\frac{1}{2}$ inch diameter by $12\frac{1}{4}$ inches long rotors operating in ambient air to a maximum compressibility number of 45. The rotors containing herringbone-groove patterns at two locations and were operated vertically in two cylindrical bronze sleeves. No external load was applied to the bearings.

1. Test results in low and high clearance sleeves indicate that half frequency whirl (HFW) is most affected by the radial clearance. The five partially grooved rotors ran stably to maximum speeds of 55,000 to 59,000 rpm when clearances ranged from 370 to 500 microinches. When clearances were increased from 550 to 710 microinches, all five rotors experienced HFW.

2. Limited test results with two rotors having identical groove geometry except for groove length and comparable clearances indicate that a fully grooved bearing is more stable than a partially grooved one. The partially grooved rotor A-1 exhibited HFW at a speed of 27,900 rpm while the fully grooved one B-1 ran to a maximum speed of 60,830 rpm without experiencing HFW.

3. Reasonably good agreement between the experimental results and existing stability criteria was obtained. The stability analysis appears to be conservative in predicting ranges of unstable operation.

4. It was shown experimentally that a region of unstable operation (HFW) can be passed through without experiencing a sizable growth in the orbital amplitude if the rotor mass parameter $\overline{M}$ is kept small.

5. Within the range of helix angles and number of grooves investigated, no significant difference in stability was observed.

APPENDIX - STABILITY CRITERION FOR JOURNAL BEARING

Stability limits for unloaded journal bearings may be found from the solutions for steady whirling of the bearing or journal (ref. 11). According to the theory, a bearing is neutrally stable when the tangential force F_t is zero and the centrifugal force due to whirling $Me\omega_3^2$ is exactly balanced by the radial bearing force F_r (fig. 9). The analysis used to find steady-state operating characteristics (ref. 9) includes a term for steady whirling. Thus, one needs only to find the whirl frequencies ω_3 for which the tangential force is zero. The whirling mass whose centrifugal force is just balanced by the radial bearing force is the critical mass M_C for this condition. In dimensionless form

$$\frac{M_C}{LD}\left(\frac{C}{R}\right)^5 \frac{RP_a}{\mu^2} = \frac{36}{\Lambda^2} \frac{F_r}{\epsilon P_a LD}\left(\frac{\omega}{\omega_3}\right)^2$$

The bearing will be stable for values of M incrementally less than M_C if the derivative of tangential force with whirl frequency $\partial F_t/\partial\omega_3$ is negative; the bearing will become unstable for M incrementally greater than M_C. The reverse holds if $\partial F_t/\partial\omega_3 > 0$.

REFERENCES

1. W. L. Stewart, W. J. Anderson, D. T. Bernatowicz, D. C. Guentert, D. E. Packe, and H. E. Rohlik, "Brayton Cycle Technology," Space Power Systems Advanced Technology Conference, NASA SP 131, 1966, pp. 95-145.

2. P. W. Curwen, A. Frost, and E. B. Arwas, "Gas Bearing Systems for NASA Solar Brayton Cycle Axial Flow Turbocompressor and Turboalternator," presented at ASME Spring Lubrication Symposium, New York, June 9, 1965.

3. B. Sternlicht, H. Poritsky, and E. Arwas, "Dynamic Stability Aspects of Cylindrical Journal Bearings Using Compressible and Incompressible Fluids," First International Symposium on Gas Lubricated Bearings, Office of Naval Research, 1959, pp. 119-160.

4. B. Sternlicht, and L. W. Winn, "Geometry Effects on the Threshold of Half-Frequency Whirl in Self-Acting, Gas-Lubricated Journal Bearings," Journal of Basic Engineering, vol. 86, no. 2, June, 1964, pp. 313-320.

5. V. N. Constantinescu, "On Hydrodynamic Instability of Gas-Lubricated Journal Bearing," Journal of Basic Engineering vol . 87, no. 3, September, 1965, pp. 579-588.

6. C. T. Pan and B. Sternlicht, "Comparison Between Theories and Experiments for the Threshold of Instability of Rigid Rotor in Self-Acting, Plain-Cylindrical Journal Bearing," Journal of Basic Engineering vol. 86, no. 2, June, 1964, pp. 321-327.

7. O. Pinkus, "Sleeve Bearing Design," Product Engineering, vol. 26, no. 8, August, 1955, pp. 134-139.

8. E. G. Gunter, Jr., J. G. Hinkle, and D. D. Fuller, "The Effects of Speed, Load, and Film Thickness on the Performance of Gas-Lubricated, Tilting-Pad Journal Bearings," ASLE Transactions, vol. 7, no. 4, October, 1964, pp. 353-365.

9. J. H. Vohr and C. Y. Chow, "Characteristics of Herringbone-Grooved, Gas-Lubricated Journal Bearings," Journal of Basic Engineering, vol. 87, no. 3, September, 1965, pp. 568-578.

10. S. B. Malanoski, "Experiments on an Ultra-Stable Gas Journal Bearing," Journal of Lubrication Technology, vol. 89, no. 4 October, 1967, pp. 433-438.

11. C. H. T. Pan, "Spectral Analysis of Gas Bearing Systems for Stability Studies," Mechanical Technology Inc. Report MTI-64-TR58, December 15, 1964. (Available from DDC as AD-610870.)

TABLE I. - TEST RESULTS OF HERRINGBONE-GROOVED ROTORS

[Groove-width to total-width ratio, 0.5; groove-length to total-bearing-length ratio, 0.6; total rotor weight, 6.06 lb (2.75 kg); rotor length, 12.25 in. (31.1 cm); bearing span, 6.64 in. (16.9 cm); nominal rotor diameter, 1.5 in. (3.8 cm); bearing length to diameter ratio, 1.0.]

Rotor number	Helix angle β, deg	Number of grooves n	Ratio of groove clearance to ridge clearance, H	Groove depth, (a)		Zero-speed radial clearance, (b)		HFW threshold speed N_s, rpm	Maximum rotor speed, rpm	Remarks
				μin.	μm	μin.	μm			
High clearances										
A-1	30	20	2.1	580	14.7	550	14.0	27 900	[c]56 500	Bounded whirl orbit, no HFW above 48 000 rpm
A-2	35	20	2.0	640	16.2	620	15.7	15 700	18 250	Unstable HFW orbit grows rapidly with increasing speed
A-3	35	23	1.9	540	13.7	600	15.2	22 300	24 130	
A-4	40	23	2.1	610	15.5	580	14.7	20 900	21 700	
A-5	40	28	2.0	710	18.0	710	18.0	14 750	16 000	
[d]B-1	30	20	1.6	330	8.4	530	13.5	------	[c]60 830	No HFW observed
Low clearances										
A-1	30	20	2.6	580	14.7	370	9.4	------	[c]55 000	Stable operation to maximum speed
A-2	35	20	2.4	640	16.2	470	11.9	------	[c]59 000	
A-3	35	23	2.5	540	13.7	350	8.9	------	[c]56 200	
A-4	40	23	2.6	610	15.5	390	9.9	------	[c]55 000	
A-5	40	28	2.4	710	18.0	500	12.7	------	[c]59 000	

[a]Depth measured with surface profile tracer (readings averaged).

[b]Assembled clearance measured at zero speed.

[c]Limiting speed with air turbine drive.

[d]Fully grooved, $Y = L_1/L = 1.0$.

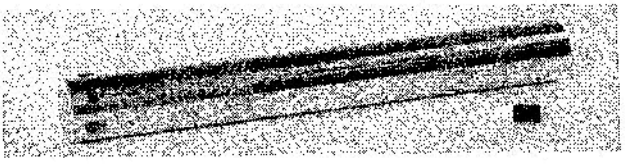

C-67-1121

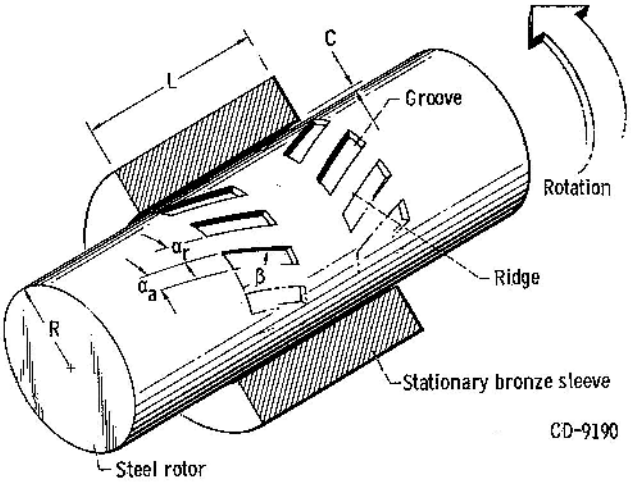

(a) Partially grooved rotors A-1 to A-5.

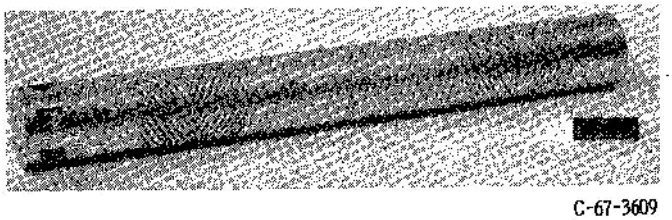

C-67-3609

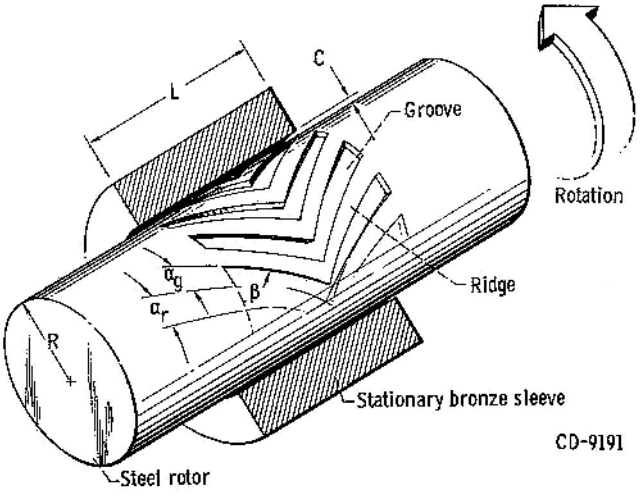

(b) Fully grooved rotor B-1.

Figure 1. - Herringbone-groove bearings.

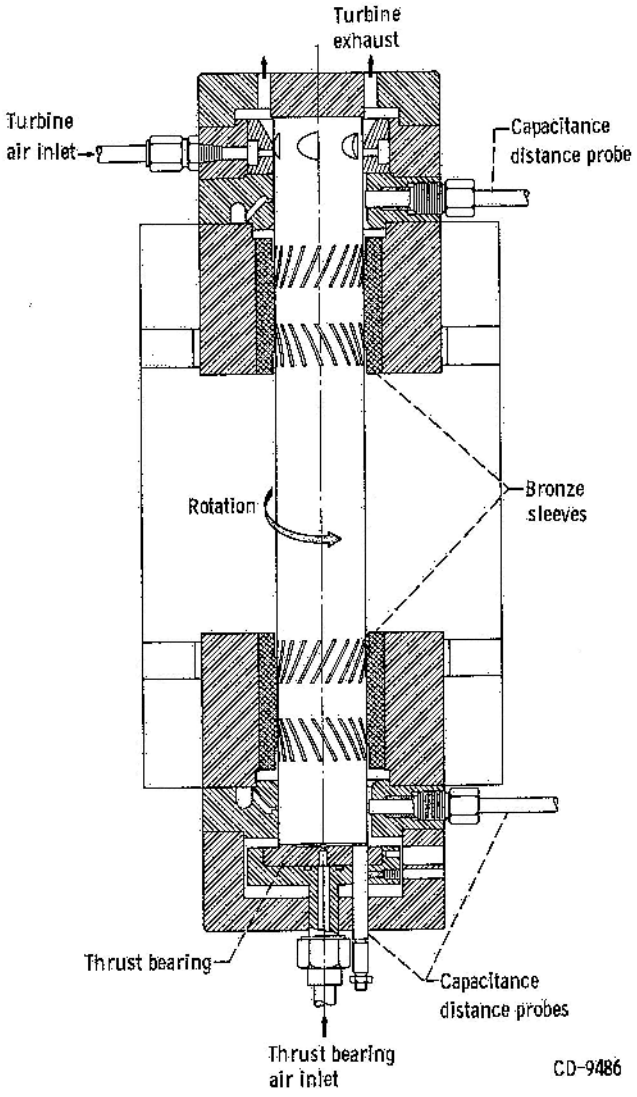

Figure 2. - Schematic drawing of thrust apparatus.

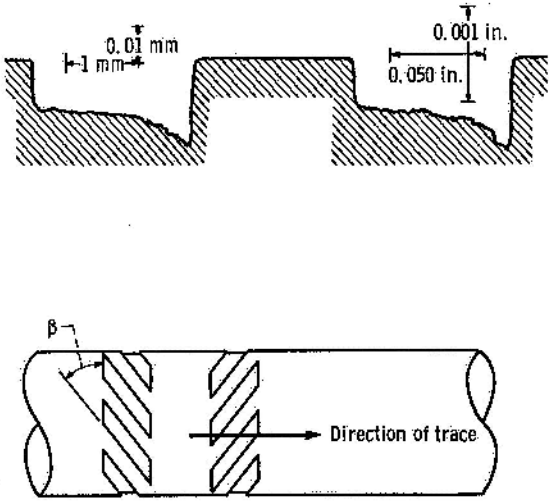

Figure 3. - Typical surface profile and trace and representation of helical grooves on rotor.

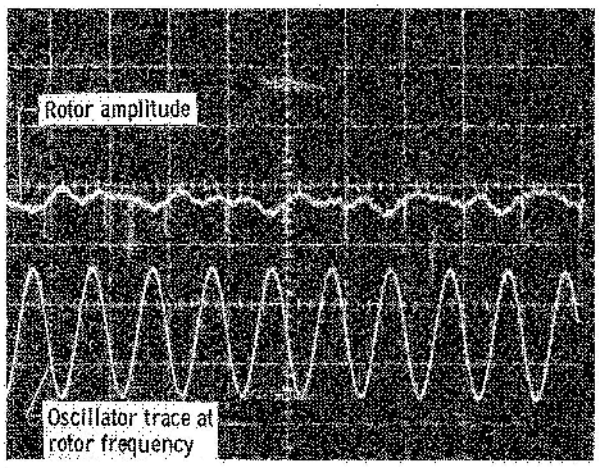

(a) Upper amplitude time trace is synchronous rotor motion at 12 000 rpm. Amplitude is 4.5 μ in. Lower trace is reference oscillator trace at rotor frequency.

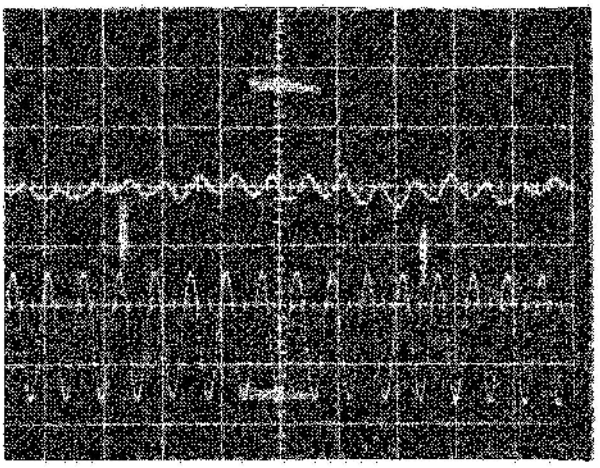

(b) Upper amplitude-time trace is synchronous rotor motion at 20 000 rpm. Amplitude is 6 μ in. Lower trace is reference oscillator trace at rotor frequency.

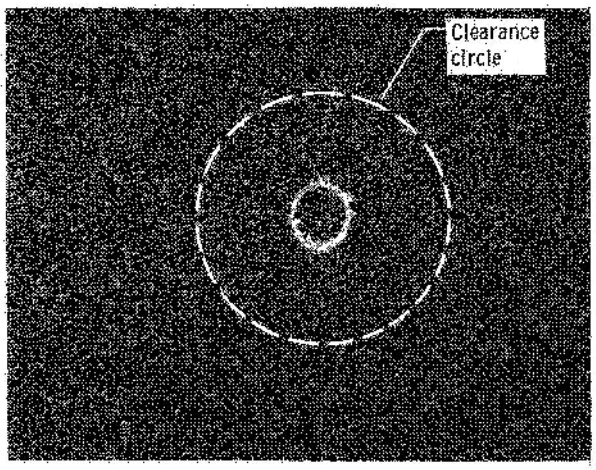

(c) X-Y trace of rotor motion in HFW at a rotor speed of 30 000 rpm. Diameter of orbit is 275 μ in.

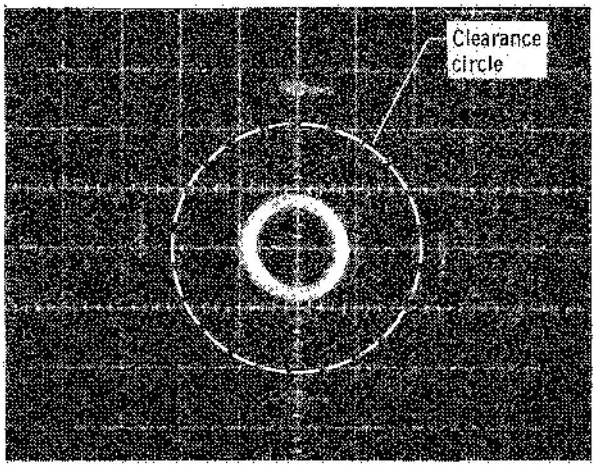

(d) X-Y trace of rotor motion in HFW at a rotor speed of 35 000 rpm. Diameter of orbit is 413 μ in.

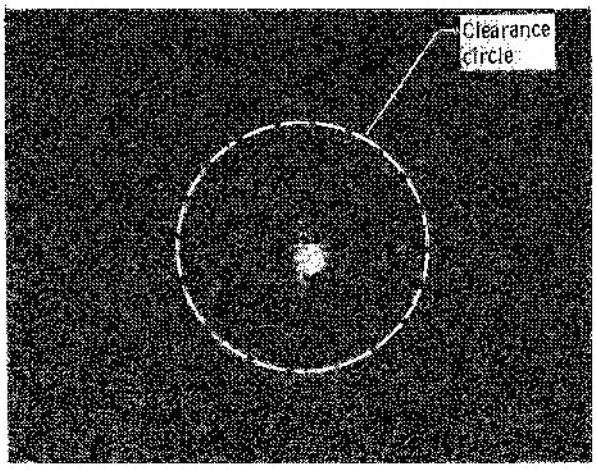

(e) X-Y trace of synchronous rotor motion at 50 000 rpm. Amplitude is 75 μ in.

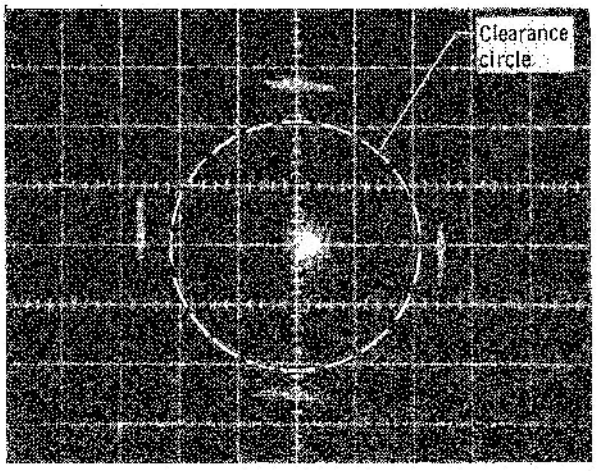

(f) X-Y trace of synchronous rotor motion at 55 230 rpm. Amplitude is 75 μ in.

Figure 4. - Motion of herringbone grooved rotor A-1 in high clearance bearing sleeves. Helix angle, $\beta = 30°$; number of grooves = 20; $H = 2.1$; $Y = 0.6$; $\alpha = 0.5$; $C = 550$ microinches (at zero speed).

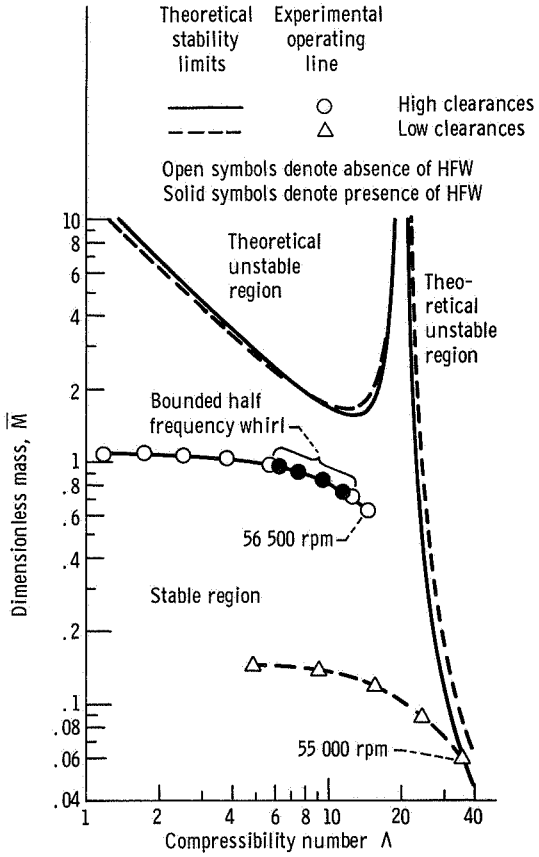

Figure 5. - Comparison of theoretical and experimental stability data for rotor A-1.

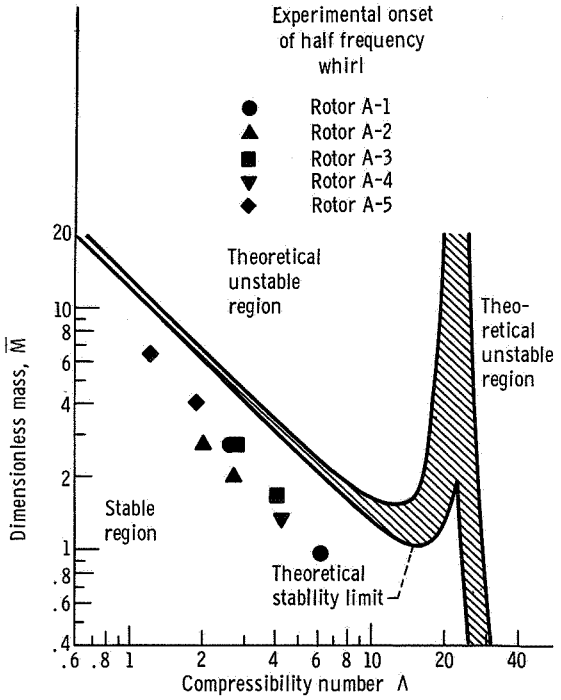

Figure 6. - Composite stability map for rotors A-1 through A-5 in high clearance bearings.

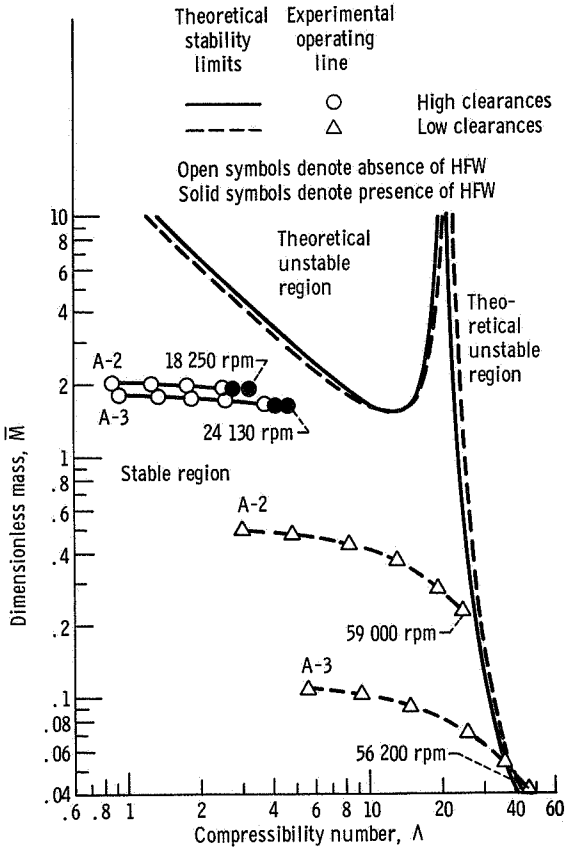

Figure 7. - Comparison of theoretical and experimental stability data for rotors A-2 and A-3.

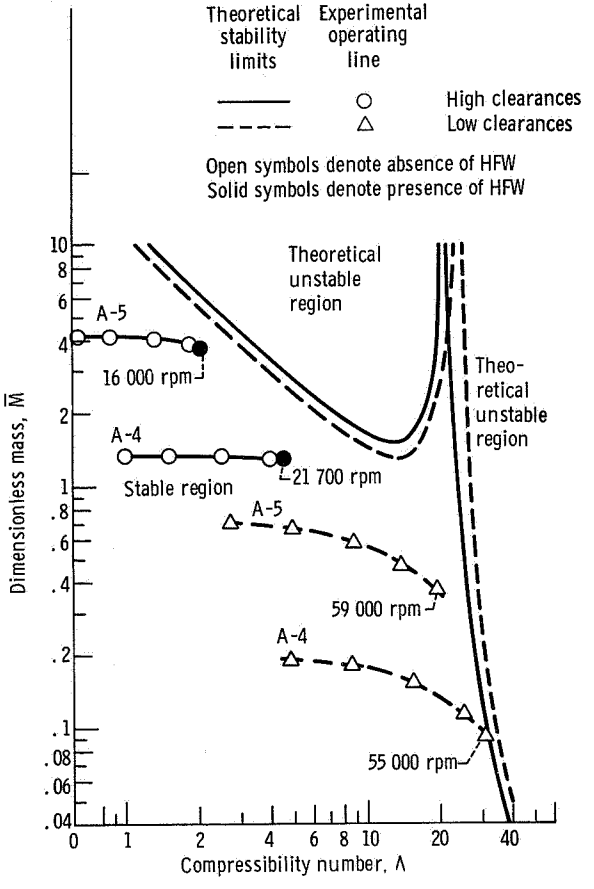

Figure 8. - Comparison of theoretical and experimental stability data for rotors A-4 and A-5.

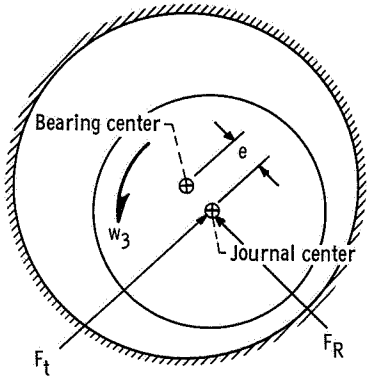

Figure 9. - Steady-state whirling of journal bearing.

NASA-CLEVELAND, OHIO E-3992